DEVELOPMENTAL DYNAMICS 237:2430–2437, 2008

RESEARCH ARTICLE

Kv11.1 Channel Subunit Composition Includes MinK and Varies Developmentally in Mouse Cardiac Muscle

Xun Wang,[1] Rongzuo Xu,[1] Grant Abernathey,[1] Jordan Taylor,[1] M.B. Alzghoul,[2] Kevin Hannon,[1] Gregory H. Hockerman,[3] and Amber L. Pond[1]*

The Kv11.1 (also ERG1) K^+ channel underlies cardiac I_{Kr}, a current that contributes to repolarization in mammalian heart. In mice, I_{Kr} current density decreases with development and studies suggest that changes in the structure and/or properties of the heteromultimeric I_{Kr}/Kv11.1 channel are responsible. Here, using immunohistochemistry, we report that total Kv11.1 α subunit protein is more abundant in neonatal heart and is distributed throughout both adult and neonatal ventricles with greater abundance in epicardia. Immunoblots reveal that the α subunit alternative splice variant, Kv11.1a, is more abundant in adult heart while the Kv11.1b variant is more abundant in neonatal heart. Additionally, MinK channel subunit protein is shown to co-assemble with Kv11.1 protein and is more abundant in neonatal heart. In summary, Kv11.1/I_{Kr} channel composition varies developmentally and the higher I_{Kr} current density in neonatal heart is likely attributable to higher abundance of Kv11.1/I_{Kr} channels, more specifically, the Kv11.1b splice variant. *Developmental Dynamics 237:2430–2437, 2008.* © 2008 Wiley-Liss, Inc.

Key words: Kv11.1; Merg1a; MinK channel; potassium channel; cardiac ion channel

Accepted 22 June 2008

INTRODUCTION

The *human ether-a-go-go–related gene* (*hKv11.1*, also *HERG* and *hKCNH2*) encodes a K^+ channel that has been identified as the locus of Long QT Syndrome 2, a disorder associated with delayed repolarization of the cardiac action potential and subsequent arrhythmias (Curran et al., 1995; Sanguinetti et al., 1995). The *hKv11.1* channel underlies native I_{Kr} current, which is partially responsible for cardiac repolarization in numerous mammals, including humans and embryonic and neonatal mice (Curran et al., 1995; Liu and Antzelevitch, 1995; Wang and Duff, 1996). Heterologous expression of *hKv11.1* produces K^+ currents that are very similar to native I_{Kr} (Trudeau et al., 1995; Zhou et al., 1998), yet differ in gating (Yang et al., 1994; London et al., 1997; Wang et al., 1997), single-channel conductance (Shibaski, 1987; Zhou et al., 1997), regulation by external K^+ (Yang et al., 1995; Yang and Roden, 1996), and sensitivity to some antiarrhythmic drugs (Follmer and Colatsky, 1990; Sanguinetti and Jurkiewicz, 1990). These differences prompted the suggestion that hKv11.1 proteins assemble with another subunit to produce I_{Kr} (Yang et al., 1995). Support for this premise has been provided by numerous studies of the association of hKv11.1 proteins with protein products of the *KCNE* gene family. These studies generally demonstrate that Kv11.1 protein associates with *KCNE* family gene products in heterologous systems to produce varied effects on channel kinetics (Yang et al., 1995; McDonald et al., 1997) and provide supportive evidence of native affiliations between *Kv11.1* and *KCNE* gene products, specifically in cardiac tissue of horse and rat (Finley

[1]Department of Basic Medical Sciences, Purdue University, West Lafayette, Indiana
[2]Department of Basic Medical Veterinary Science, Jordan University of Science and Technology, Irbid, Jordan
[3]Department of Medicinal Chemistry and Pharmacology, Purdue University, West Lafayette, Indiana
Grant sponsor: American Heart Association; Grant number: 0235363N.
***Correspondence to: Amber L. Pond, Purdue University School of Veterinary Medicine, 625 Harrison Street, G193C Lynn Hall, West. West Lafayette, IN 47906. E-mail: pond@purdue.edu**

DOI 10.1002/dvdy.21671
Published online 26 August 2008 in Wiley InterScience (www.interscience.wiley.com).

et al., 2002; Anantharam and Abbott, 2005). Furthermore, alternative splice variants of *Kv11.1* have been cloned from both human (*hKv11.1a* and *hKv11.1b*; also *HERG1A*, *HERG1B*) and mouse (*mKv11.1a* and *mKv11.1b*; also *MERG1a*, *MERG1b*) cDNA libraries (Lees-Miller et al., 1997; London et al., 1997). Currents from *Xenopus* oocytes heterologously co-expressing *mKv11.1a* and *1b* resemble native I_{Kr} more than currents produced by heterologous expression of each variant alone (London et al., 1997). However, initial studies with Kv11.1 antibodies in cardiac tissue from adult humans, rats, and mice revealed the Kv11.1a variant protein only (Pond et al., 2000). Nonetheless, knockout of the *mKv11.1b* variant eliminated the rapidly deactivating component of I_{Kr} in fetal mouse cardiomyocytes and both components of I_{Kr} from adult ventricular myocytes (Lees-Miller et al., 2003). Obviously, these results suggest that the Kv11.1b variant protein plays an important role in native I_{Kr}. Recently, studies with variant-specific and nonspecific antibodies demonstrated that, indeed, Kv11.1a and 1b proteins co-assemble to produce native I_{Kr} channels in adult cardiac tissue of rat, dog, and human (Jones et al., 2004).

I_{Kr} is the major delayed rectifier cardiac current detected during mouse embryogenesis (Wang and Duff, 1996; Wang et al., 1996) and is detected in postnatal days 1–3 (Nuss and Marban, 1994; Wang et al., 1996), although it is detected only at very low levels in adults (Wang et al., 1996; Babij et al., 1998). Furthermore, studies using ^{3}H-dofetilide (a specific I_{Kr} blocker) to measure binding sites (Kv11.1 channel) in mice revealed that, although the number of binding sites did not change from fetus through day 3 postpartum, the binding affinity declined significantly (Wang et al., 1996). These data, plus the fact that the Kv11.1 protein is abundant in adult mice (Pond et al., 2000), despite the significant decline in I_{Kr} current, suggest that the binding site is altered rather than down-regulated. Perhaps the composition and/or properties of the I_{Kr} channel are altered after neonatal day 3 and remain so throughout adulthood in normal physiological conditions.

The experiments described here were designed to explore the mKv11.1 channel subunit composition and distribution at two different developmental stages in an attempt to elucidate the mechanism(s) responsible for the reported developmental decline in I_{Kr} current densities in mice. Here we report that, although total Kv11.1 protein is more robust in neonatal heart, it is distributed throughout the atria and ventricles of both stages with greater abundance in the epicardia of the ventricles where I_{Kr} density is reported to be highest (Obreztchikova et al., 2006; reviewed in Nerbonne and Kass, 2005). Importantly, the alternative splice variant ratio, Kv11.1a:1b, varies developmentally with adult cardiac tissue containing a greater abundance of mKv11.1a than 1b protein while neonatal tissue contains more mKv11.1b than 1a protein. Also, we show that MinK protein co-immunoprecipitates with mKv11.1a protein in adult mouse heart and that MinK protein is more abundant in neonatal than in adult mouse cardiac tissue. Considering these data and the fact that knockout of mKv11.1b greatly decreased I_{Kr} expression in adult mice and deleted a component of I_{Kr} in neonatal mice (Lees-Miller et al., 2003), we suggest that a higher level of mKv11.1 protein, specifically the Kv11.1b alternative splice variant, in neonatal tissue contributes to the reported greater I_{Kr} current density in this tissue. Furthermore, because MinK has been shown to augment I_{Kr} current (Yang et al., 1995), it may contribute to increased I_{Kr} density in neonatal heart, specifically in the conductive tissue of neonates where MinK expression is reported to be restricted (Kupershmidt et al., 1999).

RESULTS

Kv11.1 Protein Is Distributed Throughout Neonatal and Adult Cardiac Tissues

Immunohistochemistry reveals that mKv11.1 protein is distributed throughout both adult and neonatal ventricles (Fig. 1A,B) and that the intensity of the immunostaining throughout these tissues is homogeneous with the exception of increased staining intensity in the epicardial layers (Fig. 1A–C) of both tissues. (The epicardial staining density is increased above that of artificially created surfaces in tissue sections [data not shown] to ensure that the staining is not artifact.) High magnification images of concurrently immunostained neonatal and adult ventricular sections (Fig. 1D) confirm that there is more mKv11.1 protein in the neonatal ventricles than in those of the adult. Consistently, immunostaining reveals a greater abundance of mKv11.1 protein in the atria relative to the ventricles of both developmental stages (Fig. 1A,B).

mKv11.1 Protein Isoform Levels Differ in Neonatal and Adult Cardiac Tissue

Western blot analyses of heart membrane protein samples, reveal the two differentially glycosylated forms of mKv11.1a protein (165 and 205 kDa) in mouse brain (Fig. 2A) and in both neonatal and adult mouse heart (Fig. 2B,C) as described earlier (Pond et al., 2000). The analyses also reveal an mKv11.1 protein at ~114 kDa and a Kv11.1 doublet at ~95 kDa. These lower mass proteins are confirmed as mKv11.1b by Western blot analysis (Fig. 2B) of concentrated membrane protein samples using the "pan" Kv11.1 antibody (Pond et al., 2000) and a specific Kv11.1b antibody (Jones et al., 2004). It is likely that the ~114-kDa protein and the ~95-kDa doublet represent mKv11.1b protein that has been posttranslationally modified. Of interest, mKv11.1a protein levels are significantly higher in adult than in neonatal heart while mKv11.1b protein levels are significantly higher in the neonatal tissue (Fig. 2C, Table 1). Specifically, the neonatal cardiac tissue contains more of the 95-kDa doublet than does the adult. Loading controls (actin protein, Fig. 2D) show that equal amounts of protein were loaded into the lanes (see note in Western blotting portion of the Experimental Procedures section).

mKv11.1 mRNA Is More Abundant in Neonatal Than Adult Hearts

We wanted to confirm the expression of mKv11.1 alternative splice variants

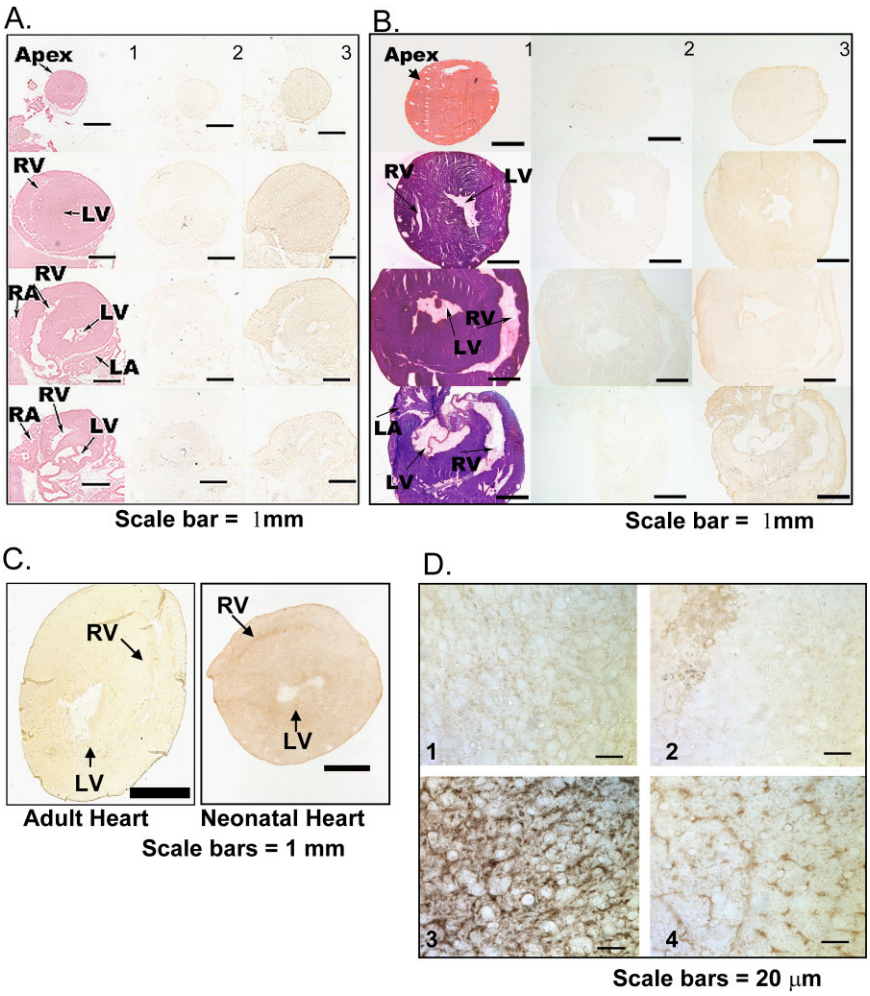

Fig. 1. Immunohistochemistry shows that mKv11.1 protein is distributed throughout the ventricles of both adult (8–9 weeks old) and neonatal (postnatal day 3) mice and is more abundant in neonatal tissue. **A:** Representative serial cross-sections from neonatal heart (1) stained with hemotoxylin and eosin, (2) immunostained without primary antibody as control, and (3) immunostained with Kv11.1 antibody. **B:** Representative serial cross-sections from adult heart (1) stained with hemotoxylin and eosin, (2) immunostained without primary antibody as control, and (3) immunostained with Kv11.1 antibody. **C:** Cross-sections from adult and neonatal ventricles concurrently immunostained for Kv11.1 protein show that total mKv11.1 protein is more abundant in the epicardial regions. **D:** High magnification of adult (panels 1 and 2) and neonatal (panels 3 and 4) heart cross-sections immunostained with (1 and 3) and without (2 and 4 as control) Kv11.1 antibody show that total mKv11.1 protein is more abundant in neonatal than adult mouse heart. Sections are representative of 12 adult hearts and 10 neonatal hearts all of which were sectioned and immunostained with "pan" Kv11.1 antibody (Pond et al., 2000).

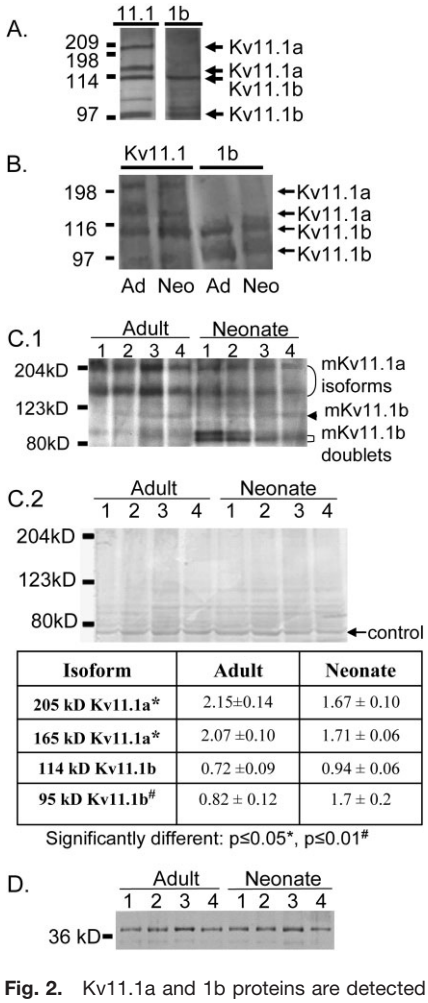

Fig. 2. Kv11.1a and 1b proteins are detected in adult and neonatal mouse tissues. Transferred membrane proteins were immunoblotted with either "pan" Kv11.1 (Pond et al., 2000) or Kv11.1b antibody (Jones et al., 2004). **A:** Kv11.1a and 1b proteins are detected in adult mouse brain. The immunoblot represents two separate blots of two different samples (five pooled brains each; 15 μg of protein per lane). **B:** mKv11.1a and 1b are expressed in mouse heart. Concentrated adult (Ad) and neonatal (Ne) samples were immunoblotted with either "pan" Kv11.1 or Kv11.1b antibody. Results represent two immunoblots of two different adult (eight pooled hearts each) and two different neonatal (~1.0 g of pooled hearts each) samples. **C.1:** Kv11.1a isoforms are more abundant in adult heart; Kv11.1b isoforms are more abundant in neonatal heart. Western blot: adult samples, lanes A1–A4 (60 μg). Neo-natal samples, lanes N1–N4, (60 μg). The immunoblot shown represents three blots of different samples (adult = nine samples of eight pooled hearts each; neonate = five samples of ~1.0 g of hearts each). **C.2:** Coomassie staining of polyvinylidene difluoride membranes confirms that each lane received equal protein. Table. Ratios of Kv11.1 protein optical densities (OD) to the OD of the lane-matched Coomasie stained control protein (± standard error of the mean) were determined and compared (Student's *t*-test). **D:** Loading controls (actin) demonstrate that each lane received equal protein.

in mouse heart and determine the relative expression levels of each of these isoforms in adult compared with neonatal mouse heart. Originally, we intended to use actin as an internal standard for RNA analyses; however, we found that adult and neonatal mouse heart samples do not contain consistently equivalent abundances of actin mRNA. Therefore, we decided to avoid potential developmental regulation of any internal control by comparing samples on a per mass RNA basis. So, to reliably compare samples, we first confirmed that the samples we wanted to compare had equal concentrations of RNA. First, we calculated the RNA concentration of each sample using optical densities and then compared the ultraviolet intensity of aliquots (containing equal RNA concentration) electrophoresed through ethidium bromide agarose gels to confirm our optical density readings (Fig. 3A). In terms of mRNA expression, rt-PCR studies show that both mKv11.1a and 1b message are detected in neonatal and adult heart (Fig. 3B,C). To allow for

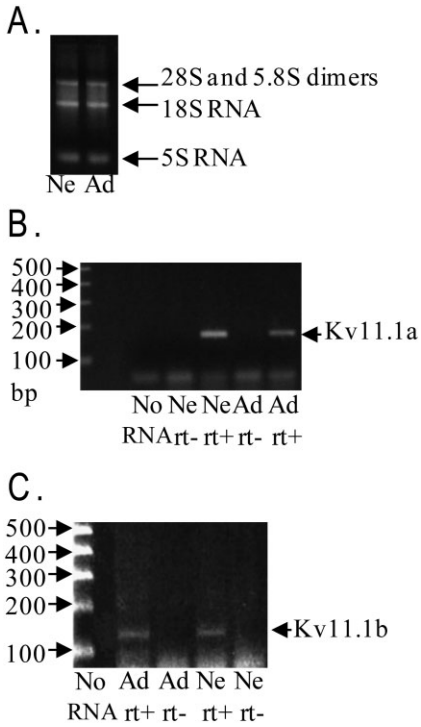

Fig. 3. Mouse Kv11.1a and 1b mRNA is detected in both adult and neonatal cardiac tissues by reverse transcriptase-polymerase chain reaction (rt-PCR) analyses. **A:** Concentrations of heart total RNA were determined and equal amounts of adult (Ad) and neonatal (Ne) total RNA were loaded onto agarose gels. The figure represents data from three adult (~two pooled hearts each) and three neonatal (~0.5 g pooled hearts each) total RNA samples each analyzed in triplicate. **B:** rt-PCR analyses show that mKv11.1a cDNA is detected in total RNA samples from adult and neonatal heart treated with reverse transcriptase (rt+). The PCR products are absent from samples not treated with reverse transcriptase (rt−) and control samples lacking mRNA template (no mRNA), indicating that the product is an amplified reverse transcriptase product. **C:** mKv11.1b cDNA is detected in total RNA samples from adult and neonatal heart treated with reverse transcriptase (rt+). No Kv11.1b mRNA is detected in samples not treated with reverse transcriptase (rt−). B and C are representative of rt-PCR analysis performed with four different adult and three different neonatal heart samples. Each of these seven samples was subjected to rt-PCR analysis in triplicate.

more accurate comparisons of mRNA levels within a gene (that is, to compare 1a levels in adult to 1a levels in neonates; and 1b levels in adult to 1b levels in neonates), we performed relative abundance studies using real-time polymerase chain reaction (PCR) in which we normalized the neonatal data to the adult data (see Experimental Procedures section). These studies reveal that neonatal heart contains 1.9 ± 0.3 (mean ± standard error of the mean) times more mKv11.1a mRNA than adult heart (n = 8 total samples, four adult and four neonatal preparations). Also, we report that neonatal heart contains 5.6 ± 1.6 (mean ± standard error of the mean) times more mKv11.1b mRNA than adult heart (n = 9, 5 adult and 4 neonatal samples).

MinK Protein Co-assembles With mKv11.1 Protein in Adult Heart

Immunoprecipitation of Kv11.1 protein also pulled down mature MinK protein as detected by Western blot of the immunoprecipitated proteins with a specific MinK antibody (Fig. 4A,B). Only a 23-kDa form of MinK was detected in the sample of protein immunoprecipitated with the "pan" Kv11.1 antibody (Fig. 4B).

MinK Protein Is More Abundant in Neonatal Than in Adult Cardiac Tissue

Western blot analyses of adult and neonatal cardiac tissues with a MinK antibody (Liu et al., 2007) revealed two isoforms of MinK: one of approximately 23 kDa and a second, much less abundant (likely nonglycosylated, "immature"; Liu et al., 2007) isoform at roughly 16 kDa (Fig. 4C). Protein band densities (corrected for potential loading errors) show that MinK protein is more abundant in neonatal than in adult mouse heart (Fig. 4C, Table 1). Loading controls (Fig. 4D) show that equal amounts of protein were loaded into each lane.

DISCUSSION

In agreement with reports from other species (Brahmajothi et al., 1997, 1999), our work demonstrates that mKv11.1 protein is distributed throughout the ventricles of both the neonatal and adult mouse hearts with more abundant protein detected in the epicardia of both developmental stages. These data correspond well with papers reporting greater I_{Kr} current densities and shorter action potential durations in this region (Obreztchikova et al., 2006; reviewed in Nerbonne and Kass, 2005). Additionally, Kv11.1 protein is distributed throughout adult and neonatal

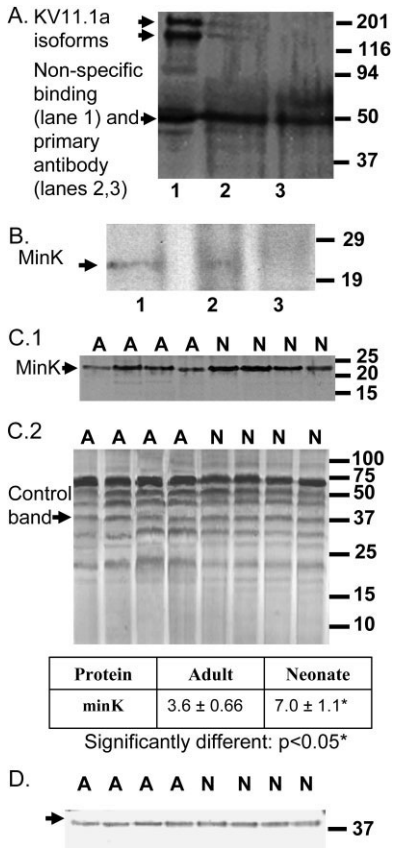

Protein	Adult	Neonate
minK	3.6 ± 0.66	7.0 ± 1.1*

Significantly different: p<0.05*

Fig. 4. MinK protein co-immunoprecipitates with mKv11.1a in adult mouse heart and is more abundant in neonatal than adult heart. **A:** Kv11.1a proteins were immunoprecipitated from adult heart (McCrossan et al., 2003), and the resultant sample was split. One half was immunoblotted (7.5% acrylamide) with Kv11.1 antibody (Pond et al., 2000). Lane 1 = adult heart; lane 2 = adult heart immunoprecipitated with Kv11.1 antibody; lane 3 = adult heart subjected to immunoprecipitation process without Kv11.1 antibody (control). **B:** MinK protein co-immunoprecipitates with Kv11.1a . Membrane proteins (from the second part of the split immunoprecipitated with Kv11.1 antibody) were electrophoresed through a 4–20% acrylamide gradient gel and immunoblotted with Kv11.1 antibody. Lane 1 = adult heart; lane 2 = adult heart protein immunoprecipitated with MinK antibody; lane 3 = adult heart subjected to immunoprecipitation without Kv11.1a antibody. The co-immunoprecipitation (Fig. 4A, B) was done thrice. **C.1:** More abundant MinK protein is detected in neonatal (N, 40 μg) relative to adult (A, 40 μg) heart. Membrane proteins were electrophoresed (as above), transferred, and immunoblotted with MinK antibody (Liu et al., 2007). This blot (eight samples) was done twice. **C.2:** Coomassie staining of polyvinylidene difluoride membranes confirm that equal amounts of protein were loaded. Table: Ratios of MinK protein optical density (OD) to the OD of the lane-matched Coomassie stained control protein (± standard error of the mean) were determined and compared (Student's *t*-test). **D:** Loading controls (actin) demonstrate that each lane received equal protein.

atria with greater abundance in atria than in ventricles as shown earlier in rats (Pond et al., 2000). Immunohistochemistry data reveal that Kv11.1 protein is more abundant in neonatal than in adult heart which is not surprising because higher I_{Kr} density is reported in the hearts of neonatal mice (Wang and Duff, 1996; Wang et al., 1996).

In agreement with recent work in humans, dogs, and rats (Jones et al., 2004), we find both Kv11.1a and 1b alternative splice variants in adult and neonatal mouse heart; however, this contradicts our earlier study reporting detection of solely the mKv11.1a variant in adult rat and human heart (Pond et al., 2000). We suggest that we did not detect the mKv11.1b isoform earlier because we were working with adult mouse tissues in which mKv11.1b protein is not as abundant; therefore, the mKv11.1b proteins were not consistently obvious in our immunoblots. Our current study, using a "pan" Kv11.1 antibody, reveals the two Kv11.1a protein isoforms (205 and 165 kDa) reported earlier (Pond et al., 2000) and two Kv11.1b protein isoforms (114 and 95 kDa) in mouse heart membrane proteins. The number of isoforms detected in mice is similar to those detected in rat by the Robertson laboratory (Jones et al., 2004), although the reported molecular masses are different. Because our earlier studies (Pond et al., 2000; Wang et al., 2006) show that our "pan" Kv11.1 antibody is specific for Kv11.1 proteins, we suggest that these differences in Kv11.1 isoform molecular masses likely result from species-specific differences in posttranslational modification; alternatively, these could result from differences in the protocols used in membrane protein sample preparation and immunoblotting. Nonetheless, our Western blots show that mKv11.1a proteins are significantly more abundant in adult than in neonatal heart; however, there is no significant difference in abundances of the ~114-kDa mKv11.1b protein. Yet, when optical densities (corrected for potential loading errors) of the 1a isoforms and this 1b protein are compared, the ~114-kDa 1b protein is significantly less abundant than the 1a isoforms in both adult and neonatal heart. After exhaustive study of membrane preparations, we believe that the relative low abundance of this ~114-kDa Kv11.1b isoform truly represents a lower expression level of this variant and not degradation of this protein occurring during sample preparation. The ~95-kDa doublet could also represent degradation product(s). However, because 90 kDa is the predicted molecular mass of the mKv11.1b protein (London et al., 1997; Jones et al., 2004) and Kv11.1 channels are posttranslationally modified (Pond et al., 2000; Jones et al., 2004), it is more likely that the ~114-kDa protein and the ~95-kDa doublet proteins are posttranslationally modified (perhaps variably glycosylated) forms of mKv11.1b. Nonetheless, there is a significantly higher abundance of total mKv11.1b protein in neonatal than in adult heart while there is a significantly greater abundance of mKv11.1a protein in the adult. The data show that the ratio of mKv11.1a:1b proteins varies developmentally in mice and suggests that not all cardiac mKv11.1 channels are heteromultimers of 1a and 1b.

The varying ratios of α subunits (1a:1b) likely contribute to the developmental differences in mouse I_{Kr}, specifically current density and/or deactivation rates. Studies show that I_{Kr} densities are higher in fetal mice and decrease with age, becoming extremely low in adults (Wang and Duff, 1996; Wang et al., 1996; Babij et al., 1998). Furthermore, in studies of *Merg1b* (*Kv11.1b*) knockout mice, density of the fast component of I_{Kr} was decreased by 90% in fetal knockout mice while both the fast and slow components of I_{Kr} were abolished in the adults (Lees-Miller et al., 2003). Here we show that the Kv11.1b protein is more prominent in younger mice than adults, supporting the evidence that this subunit is important for current conduction in heart. Additionally, heterologous expression studies show that the 1b subunit deactivates at a ~10-fold faster rate than that of isoform 1a and faster than heteromultimers of 1a and 1b (Lees-Miller et al., 1997; London et al., 1997). Therefore, the developmentally different 1a:1b ratios detected here would be expected to produce developmentally different deactivation kinetics. Indeed, Lees-Miller et al. (2003) reported that the decay of I_{Kr} tail currents varies between the adult and fetal (18 day) mouse and that faster deactivation is exhibited by the adult mouse for both the fast and slow components. Because the fast deactivation rate of 1b is expected to dominate deactivation kinetics (Wang et al., 2000) and the 1b subunit is more prominent in the neonatal mouse (present study), we would expect the deactivation rate of I_{Kr} to be faster in neonatal mice, but it is not (Lees-Miller et al., 2003). These data suggest that I_{Kr} deactivation kinetics are regulated by more than the ratio of 1a and 1b subunits present in the plasma membrane.

In fact, various reports demonstrate that MinK co-assembles with Kv11.1 subunits in heterologous expression systems to modulate the Kv11.1 current (Yang et al., 1995; McDonald, 1997). Two recent reports show that MinK and mKv11.1 co-immunoprecipitate in adult rat (Anantharam and Abbott, 2005) and horse (Finley et al., 2002) heart. Here, we have detected MinK protein in cardiac membrane samples immunoprecipitated with Kv11.1 antibody. These data strongly suggest that MinK protein co-assembles with Kv11.1a in mouse tissues to regulate I_{Kr} current *in vivo* as has been shown to occur in vitro (Yang et al., 1995; McDonald et al., 1997). Indeed, this important finding supports reports that the I_{Kr} channel is composed of α and auxiliary subunits and that regional variation in I_{Kr} may result from regional differences in auxiliary subunit expression (Yang et al., 1995; Kuperschmidt et al., 1999). It is interesting that no Kv11.1b isoform was detected in the sample immunoprecipitated with the "pan" Kv11.1 antibody. It is likely that the low abundance of the Kv11.1b protein in the adult heart is preventing immunoprecipitation of detectable levels of this protein (with our current immunoprecipitation protocol). It may be possible to immunoprecipitate the Kv11.1b protein from the neonatal heart; however, collecting the amount of tissue necessary is not a trivial matter. Our data also reveal a greater abundance of MinK protein in neonatal relative to adult cardiac tissues. This is similar to developmental patterns reported for MinK mRNA and protein in mouse heart (Kondo et al., 2003; Harrell et al., 2007); however, the relative differences in the mRNA data is much more

striking than the differences in protein data. Indeed, it is not unusual for mRNA and protein data to not correlate well in terms of relative abundances. It may well be that the (transmembrane) MinK protein, has a much longer half life in cardiomyocytes than does the precursor mRNA. Furthermore, MinK has been shown to increase I_{Kr} current (Yang et al., 1995) and, therefore, may contribute to the higher I_{Kr} density in neonatal heart. This effect would be expected to be most prominent in the conductive tissue of neonates where MinK expression is reported to be restricted (Kupershmidt et al., 1999).

In summary, our data show that *mKv11.1* expression is greater in the neonatal mouse heart than in adult, and that the ratio of alternative splice variant proteins, mKv11.1a:mKv11.1b, varies developmentally. We also detect more abundant levels of MinK protein in neonatal than in adult heart and show that this protein co-assembles with mKv11.1 in mouse heart. We suggest, therefore, that the developmental differences in channel protein levels likely contribute to the developmental, regional, and subregional variations reported in I_{Kr} current. Obviously, these data do not discount the possible occurrence of any other developmental alteration in mKv11.1/I_{Kr} channel composition or regulation. Nonetheless, this study confirms that the developmental regulation of I_{Kr} current is a complicated matter dependent upon the expression of at least three different proteins: Kv11.1a, 1b and MinK.

EXPERIMENTAL PROCEDURES

Animals

All procedures were approved by the Purdue Animal Care and Use Committee. Adult (8–9 weeks old) male C57BL5 mice (Harlan-Sprague; Indianapolis, IN) were used in all procedures requiring adult tissue. Neonatal (3 days old) C57BL5 mice were bred in the Purdue facility; both male and female neonates were used. All animals were housed in Purdue University facilities, monitored by Purdue University lab animal veterinarians, and provided food and water ad libitum.

Antibodies

The Kv11.1 (erg1) (Pond et al., 2000) and MinK antibodies (Liu et al., 2007) were developed in the laboratory of Dr. Jeanne Nerbonne (Washington University, St. Louis, MO). The specific Kv11.1b (erg1b) antibody was a generous gift from Dr. Gail Robertson (University of Wisconsin, Madison; Jones et al., 2004). The actin antibody was purchased from Sigma (St. Louis, MO).

Tissue Sections and Staining

Animal hearts were embedded with OCT (Sakura; Torrance, CA) and cryosectioned (14 μm thick). Sections were immunostained using primary antibody (Pond et al., 2000) followed with horseradish peroxidase conjugated goat anti-rabbit antibody and diaminobenzidine color development per manufacturer's instructions (Sigma).

Western Blot

For immunoblots, membrane protein samples were prepared from heart and brain tissues as described previously (Pond et al., 2000). Samples described as concentrated in figure legends were centrifuged (per manufacturer's instructions) using 30-kDa molecular weight cut off Centricons (Millipore; Billerica, MA). Sample protein concentrations were determined by the Bio-Rad DC analysis (Bio-Rad; Hercules, CA). Sample aliquots (protein concentrations determined to be within a linear range of response for Western blotting) were electrophoresed through a 7.5% acrylamide gel (Figs. 2, 4A) or a 4–20% acrylamide gradient gel (Fig. 4B–D), transferred to polyvinylidene difluoride membrane, immunoblotted with antibody (as described in figure legends), and further developed with chemiluminescence (Pond et al., 2000). All membranes were exposed to film for multiple time spans to ensure that the films were not saturated before scanning for determination of optical density. After blotting, membranes were stained with 0.1% Coomassie R-250 (in 45% methanol and 10% acetic acid) and destained with 50% methanol to confirm that the membrane samples contained equal protein. Note: We detect equivalent levels of actin protein in our adult and neonatal heart samples, although we do not detect equal levels of actin mRNA. This is likely because Western blot analyses are not as sensitive as reverse transcriptase (rt) -PCR and/or because the levels of actin mRNA transcribed and levels of actin protein translated do not correlate well.

Optical Densities

Optical densities of film and membrane protein bands were determined using Optimas 6.1 (Optimas; West Malling, UK). The films and membranes were scanned and the images were loaded into the Optimas 6.1 software. An area to be measured was defined within each protein band, and the optical density (OD; that is, the mean log inverse gray value of pixels within the boundary area or ArLIGV) of each protein band was determined.

rt-PCR

Trizol reagent was used to extract total RNA from hearts. The extraction was followed by phenol/chloroform extraction and ethanol precipitation. Any contaminating DNA was degraded by two individual 10-min treatments with DNase I (Promega; Madison, WI). DNase was then heat inactivated. Duplicate samples were either exposed to reverse transcriptase (rt+) or vehicle only (rt−). The "no template" control sample did not receive any total RNA. The reverse transcription product was treated with RNaseH to remove remaining RNA and amplified with PCR using exon spanning primers for (1) mKv11.1a, 5′-CGC AGA ACA CCT TCC TCG ACA C-3′ (forward) and 5′-GCA GAA GCC GTC GTT GCA GTA G-3′ (reverse); and (2) mKv11.1b, 5′-CGC AGA ACA CCT TCC TCG ACA C-3′ (forward) and 5′-GCA GAA GCC GTC GTT GCA GTA G-3′ (reverse). This product was combined with ethidium bromide and then electrophoresed on a 2% agarose gel (Wang et al., 2006).

Relative Abundances of mRNA (Real-Time PCR)

Total mRNA was extracted and treated as above except that SYBR Green Supermix with Rox (Bio-Rad; Hercules, CA) was added to the PCR reaction (per manufacturer's instruc-

tions). The primers used are the same as described above for the rt-PCR. A 7300 Real-Time PCR System (Applied Biosystems; Foster City, CA) was used to detect SYBR Green fluorescence as a measure of amplicon. The relative abundances of Kv11.1 isoform mRNA in adult and neonatal hearts were calculated as follows: the number 2 was raised to a power equal to the difference in C_T values from the rt+ group for each sample (see equation).

Equation:

Neonate: Adult = $2^{[C_T(X \text{ of } A) - C_T(X \text{ of } B)]}$

Where: Neonate = mRNA level of gene X in neonatal sample; Adult = mRNA level of gene X in adult sample; Gene X = gene of interest (e.g., merg1a or 1b); C_T= Threshold cycle (point at which early amplification is exponential); $C_T^{(X \text{ of } A)}$ = Threshold cycle number in RT+ group for gene X in neonatal heart; $C_T^{(X \text{ of } B)}$ = Threshold cycle number in RT+ group for gene X in adult heart.

Immunoprecipitation of mKv11.1a From Adult Mouse Heart

The mKv11.1a protein was immunoprecipitated from adult mouse heart with our "pan" Kv11.1 antibody using a protocol slightly modified from one developed by Dr. Geoff Abbott (Cornell University; McCrossan et al., 2003; Anantharam and Abbot, 2005). Briefly, seven mouse hearts were homogenized in 15–20 ml of 10 mM MOPS (pH 7.4) containing 0.6 mM sucrose and protease inhibitor cocktail (Roche; Mannheim, Germany). The homogenate was centrifuged (500 × *g*, 5 min, 4°C) and the resultant supernatant was centrifuged (12,000 × *g*, 30 min, 4°C). This final supernatant was diluted to 40 ml with 20 mM MOPS (pH 7.4) containing 160 mM NaCl and protease inhibitor cocktail (as above). Sucrose (10 ml of 1 M) was added, and this was centrifuged (160,000 × *g*, 1 hr, 4°C). The pellet was resuspended in 0.7 ml of 20 mM MOPS (pH 7.4) containing (in mM) 54 LiCl, 6 KCl, 100 NaCl and protease inhibitor as above by passing the suspension through progressively smaller needles. The homogenate was then diluted 10:1 in 50 mM Tris-HCl (pH 7.4) containing 20 mM NaF, 10 mM $NaVO_4$, 1 mM phenylmethyl sulfonyl fluoride, 0.5% sodium dodecyl sulfate (SDS), 0.5% CHAPS, 1% Triton X-100, 1% Non-Idet P40, and protease inhibitor as above. The homogenate was rocked for 1 hr at 4°C, centrifuged (20,000 × *g*, 5 min, 4°C), and precleared by incubation (4°C, 30 min) with Protein A Sepharose beads (Sigma). After bead removal, the homogenate was incubated with antibody (1 μl/600 μl supernatant) overnight. The homogenate was then incubated with Protein A Sepharose beads for 5 hr. After washes, the beads were incubated in 50 mM Tris (pH 6.7) containing 1 mM ethylenediaminetetraacetic acid, 1.5% SDS, 10% glycerol, and 5% BME for 20 min at 37°C and then heated to 50°C for 20 min. SDS-polyacrylamide gel electrophoresis followed.

Statistical Analyses

Density measurements were assessed using a Student *t*-test (Steel and Torrie, 1980). All data were analyzed using the General Linear Models procedure of SAS (SAS Institute, 2003) for a completely randomized design. Statements were based on ($P \leq 0.05$) unless otherwise noted.

ACKNOWLEDGMENTS

The authors thank Dr. Gail Robertson (University of Wisconsin, Madison, WI) for the generous gift of the Kv11.1b-specific antibody and Dr. Geoffrey Abbott (Cornell University) for sharing his Kv11.1 immunoprecipitation protocol. We give special thanks to Dr. Gea-Ny Tseng (University of Virginia) for helpful discussions and Mr. Curt Sherwin for gracious help preparing images for publication. X.W. is now at the University of Michigan (Ann Arbor), J.T. is at the Washington University School of Medicine (St. Louis, MO), G.A. is at Indiana University (Indianapolis), and R.X. is at the University of Utah (Salt Lake City). A.L.P. received the supporting Scientist Development Grant from the American Heart Association.

REFERENCES

Anantharam A, Abbott GW. 2005. Does hERG coassemble with a β subunit? Evidence for roles of MinK and MiRP1. In: Novartis Foundation Symposium 266: The hERG cardiac potassium channel: structure, function and long QT syndrome. New York: John Wiley and Sons, Ltd. p 155–158.

Babij P, Askew GR, Nieuwenhuijsen B, Su CM, Bridal TR, Jow B, Argentieri TM, Kulik J, DeGennaro LJ, Spinelli W, Colatsky TJ. 1998. Inhibition of cardiac delayed rectifier K+ current by overexpression of the long-QT syndrome HERG G628S mutation in transgenic mice. Circ Res 83:668–678.

Brahmajothi MV, Morales MJ, Rasmusson RL, Campbell DL, Strauss HC. 1997. Heterogeneity in K+ channel transcript expression detected in isolated ferret cardiac myocytes. Pacing Clin Electrophysiol 20:388–396.

Brahmajothi MV, Morales MJ, Reimer KA, Strauss HC. 1999. Distinct transient outward potassium current (Ito) phenotypes and distribution of fast-inactivating potassium channel alpha subunits in ferret left ventricular myocytes. J Gen Physiol 113:581–600.

Curran ME, Splawski I, Timothy KW, Vincent GM, Green ED, Keating MT. 1995. A molecular basis for cardiac arrhythmia: HERG mutations cause long QT syndrome. Cell 80:795–803.

Finley MR, Li Y, Hua F. 2002. Expression and coassociation of ERG1, KCNQ1, and KCNE1 potassium channel proteins in horse heart. Am J Physiol Heart Circ Physiol 283:H126–H138.

Follmer CH, Colatsky TJ. 1990. Channel specificity in antiarrhythmic drug action. Mechanism of potassium channel block and its role in suppressing and aggravating cardiac arrhythmias. Circulation 82:289–293.

Harrell MD, Harbi S, Hoffman JF, Zavadil J, Coetzee WA. 2007. Large-scale analysis of ion channel gene expression in the mouse heart during perinatal development. Physiol Genomics 28:273–283.

Jones EM, Roti Roti EC, Wang J, Delfosse SA, Robertson GA. 2004. Cardiac IKr channels minimally comprise hERG 1a and 1b subunits. J Biol Chem 279:44690–44694.

Kondo RP, Anderson RH, Kupershmidt S, Roden DM, Evans SE. 2003. Development of the cardiac conduction system as delineated by mink-lacZ. J Cardiovasc Electrophysiol 14:383–391.

Kupershmidt S, Yang T, Anderson ME, Wessels A, Niswender KD, Magnuson MA, Roden DM. 1999. Replacement by homologous recombination of the minK gene with lacZ reveals restriction of minK expression to the mouse cardiac conduction system. Circ Res 84:146–152.

Lees-Miller JP, Kondo C, Wang L, Duff HJ. 1997. Electrophysiological characterization of an alternatively processed ERG K+ channel in mouse and human hearts. Circ Res 81:719–726.

Lees-Miller JP, Guo J, Somers JR, Roach DE, Sheldon RS, Rancourt DE, Duff HJ. 2003. Selective knockout of mouse ERG1 B potassium channel eliminates I(Kr) in adult ventricular myocytes and elicits

episodes of abrupt sinus bradycardia. Mol Cell Biol 23:1856–1862.

Liu D-W, Antzelevitch C. 1995. Characteristics of the delayed rectifier current (IKr and IKs) in canine ventricular epicardial, midmyocardial, and endocardial myocytes. A weaker IKs contributes to the longer action potential of the M cell. Circ Res 76:351–365.

Liu X-S, Jiang M, Zhang M, Tang D, Higgins RSD, Clemo SHF, Tseng G-N. 2007. Electrical remodeling in a canine model of ischemic cardiomyopathy. Am J Physiol Heart Circ Physiol 292:H560–H571.

London B, Trudeau MC, Newton KP, Beyer AK, Copeland NG, Gilbert DJ, Jenkins NA, Satler CA, Robertson GA. 1997. Two isoforms of the mouse ether-a-go-go-related gene coassemble to form channels with properties similar to the rapidly activating component of the cardiac delayed rectifier K+ current. Circ Res 81: 870–878.

McCrossan ZA, Lewis A, Panaghie G, Jordan PN, Christini DJ, Lerner DJ, Abbott GW. 2003. MinK-related peptide 2 modulates Kv2.1 and Kv3.1 potassium channels in mammalian brain. J Neurosci 23: 8077–8091.

McDonald TV, Yu Z, Ming Z, Palma E, Meyers MB, Wang KW, Goldstein SA, Fishman GW. 1997. A minK-HERG complex regulates the cardiac potassium current I(Kr). Nature 388:289–292.

Nerbonne JM, Kass RS. 2005. Molecular physiology of cardiac repolarization. Physiol Rev 85:1205–1253.

Nuss HB, Marban E. 1994. Electrophysiological properties of neonatal mouse cardiac myocytes in primary culture. J Physiol 479:265–279.

Obreztchikova MN, Patberg KW, Plotnikov AN, Ozgen N, Shlapakova IN, Rybin AV, Sosunov EA, Danilo P Jr, Anyukhovsky EP, Robinson RB, Rosen MR. 2006. I(Kr) contributes to the altered ventricular repolarization that determines long-term cardiac memory. Cardiovasc Res 71:88–96.

Pond AL, Scheve BK, Benedict AT, Petrecca K, Van Wagoner DR, Shrier A, Nerbonne JM. 2000. Expression of distinct ERG proteins in rat, mouse, and human heart. Relation to functional I(Kr) channels. J Biol Chem 275:5997–6006.

Sanguinetti MC, Jurkiewicz NK. 1990. Lanthanum blocks a specific component of IK and screens membrane surface change in cardiac cells. Am J Physiol 259:H1881–H1889.

Sanguinetti MC, Jurkiewicz NK. 1991. Delayed rectifier outward K+ current is composed of two currents in guinea pig atrial cells. Am J Physiol 260:H393–H399.

Shibaski T. 1987. Conductance and kinetics of delayed rectifier potassium channels in nodal cells of the rabbit heart. J Physiol 387:227–250.

Steel RGD, Torrie JH. 1980. Principles and procedures of statistics: a biomedical approach. 2nd ed. New York: McGraw-Hill. 634 p.

Trudeau MC, Warmke JW, Ganetzky B, Robertson GA. 1995. HERG, a human inward rectifier in the voltage-gated potassium channel family. Science 269:92–95.

Wang L, Duff HJ. 1996. Identification and characteristics of delayed rectifier K+ current in fetal mouse ventricular myocytes. Am J Physiol 270:H2088–H2093.

Wang J, Myers CD, Robertson GA. 2000. Dynamic control of deactivation gating by a soluble amino-terminal domain in HERG K+ channels. J Gen Physiol 115: 749–758.

Wang L, Feng Z-P, Kondo CS, Sheldon RS, Duff HJ. 1996. Developmental changes in the delayed rectifier K+ channels in mouse heart. Circ Res 79:79–85.

Wang S, Liu S, Morales MJ, Strauss HC, Rasmusson RL. 1997. A quantitative analysis of the activation and inactivation kinetics of HERG expressed in Xenopus oocytes. J Physiol 502:45–60.

Wang X, Hockerman GH, Green III HW, Bobbs CF, Mohammad SI, Gerrard D, Latour MA, London B, Hannon KM, Pond AL. 2006. Mergla K^+ channel induces skeletal muscle atrophy by activating the ubiquitin proteasome pathway. FASEB J 20:1531–1533.

Yang T, Roden DM. 1996. Extracellular potassium modulation of drug block of IKr. Implications for torsade de pointes and reverse use-dependence. Circulation 93: 407–411.

Yang T, Wathen MS, Felipe A, Tamkun MM, Snyders DJ, Roden DM. 1994. K+ currents and K+ channel mRNA in cultured atrial cardiac myocytes (AT-1 cells). Circ Res 7:870–878.

Yang T, Kupershmidt S, Roden DM. 1995. Anti-minK antisense decreases the amplitude of the rapidly activating cardiac delayed rectifier K+ current. Circ Res 77:1246–1253.

Zhou A, Curran ME, Keating MT, Sanguinette MC. 1997. Single HERG delayed rectifier K+ channels expressed in Xenopus oocytes. Am J Physiol 272:H1309–H1314.

Zhou Z, Gong Q, Ye B, Fan Z, Makielski JC, Robertson GA, January CT. 1998. Properties of HERG channels stably expressed in HEK 293 cells studied at physiological temperature. Biophys J 74: 230–241.